**NANO REVIEW**

# Electrically Doped Nanoscale Devices Using First-Principle Approach: A Comprehensive Survey

Debarati Dey[1,2], Debashis De[2,3], Ali Ahmadian[4,6*] ⓘ, Ferial Ghaemi[5] and Norazak Senu[6]

**Abstract**

Doping is the key feature in semiconductor device fabrication. Many strategies have been discovered for controlling doping in the area of semiconductor physics during the past few decades. Electrical doping is a promising strategy that is used for effective tuning of the charge populations, electronic properties, and transmission properties. This doping process reduces the risk of high temperature, contamination of foreign particles. Significant experimental and theoretical efforts are demonstrated to study the characteristics of electrical doping during the past few decades. In this article, we first briefly review the historical roadmap of electrical doping. Secondly, we will discuss electrical doping at the molecular level. Thus, we will review some experimental works at the molecular level along with we review a variety of research works that are performed based on electrical doping. Then we figure out importance of electrical doping and its importance. Furthermore, we describe the methods of electrical doping. Finally, we conclude with a brief comparative study between electrical and conventional doping methods.

**Keywords:** Electrical doping, DFT, NEGF, First principle, Molecular modeling

## Introduction

Doping plays a crucial role in determining physical characteristics and their applications of various organic or inorganic materials, especially for semiconductors. This method has been successfully proved for the semiconductor physics industry. A small amount of addition of impurities determines the dopant concentration and electrical conductivities of the materials. It is observed that an ideal dopant should exhibit an ideal solubility in its host material, and it also exhibits a low defect level. However, some basic problems are related to this type of conventional doping process, for example, doping bottleneck which powerfully affects the device performance. This type of performance degradation has been observed severely for wide bandgap materials.

For example, in the case of the minima of high conduction band device, n-type doping is challenging, whereas for maxima of the low valence band device is also complicated [1, 2]. Therefore, some problems arise for the bipolar doping process in wideband semiconductors. It is observed that either p-type or n-type dopants can be inserted but not together [3]. Therefore, to compensate for this type of problem, a feasible solution has been incorporated into the domain of doping. This type of proposed approach is known as electrical doping, which does not depend on this type of bipolar doping. Electrical doping has been introduced to solve the problems of bipolar doping. In the late 1980s' and 1990s', researchers observed that III–V compounds like a single crystal of GaN are difficult to grow. Even more, for commercial use of GaN substrates were also unavailable at the era of the late 1990s'. The reason behind it was explained in such a manner that the difference between lattice constants and coefficients of thermal expansion of the sapphire substrate and the GaN semiconductor made it difficult to grow a high-quality GaN-based epitaxial layer on the

*Correspondence: ali.ahmadian@ukm.edu.my
[4] Institute of IR 4.0, The National University of Malaysia (UKM), 43600 Bangi, Selangor, Malaysia
Full list of author information is available at the end of the article

Dey *et al. Nanoscale Res Lett*     (2021) 16:20

Page 2 of 16

sapphire substrate. On the other hand, it was almost impossible to obtain a p-type GaN semiconductor due to combinations of high n-type background concentration and low p-type doping activity. This problem can be significantly overcome using the electrical doping phenomenon by Rudaz in the year of 1998. During the late 1980s', scientists discovered the importance of growing GaN or AlN buffer layers to demonstrate GaN-based LED at low temperatures. Post-growth thermal annealing process helps to activate the growth of p-type dopants in GaN buffer layers. These advancements accelerated the growth in device development of the III–V nitride semiconductor material system for wide-band optoelectronic devices [4]. GaN substrate and post-growth thermal annealing process also play an important role in this technique [5–7]. Since last few decades, plasma etching technology plays an important role in ultra-large-scale technology (ULSI) to shrink the pattern size. This led us to the evolution of nanotechnology. On the same time, plasma technology faced some inherent problems for example; build up of charge, photon UV radiation along with etching performance for nanoscale devices. To remove these problems and fabricate practical nanoscale devices, neutral–beam etching process has come into the field. S. Samukawa has introduced this neutral beam sources and also talked about the combination of top-down and bottom-up processing for prospect nanoscale devices. Neutral beams technology is executed damage-free etching because it is used atomically. Using this technique surface modification of inorganic and organic materials can also be done. This technique is a capable contender for the practical fabrication technology for future nanodevices [8]. This high-density plasma technology includes inductively coupled plasma (ICP) and electron-cyclotron-resonance (ECR) plasma, which are the key methods for the implementations of this plasma technique. But there are several problems associated with this technique, such as

- Various types of radiation may damage the charge buildup of positive ions and electrons [8–12].
- The radiation of ultraviolet (UV), vacuum ultraviolet (VUV) ray may also damage nanoscale devices.
- X-ray photons may also cause rupture of nanoscale devices during this plasma etching problem [13–21].
- Due to charge buildup due to voltage generation distort ion trajectories, it also leads to fracture of thin gate oxide films.
- In addition to these, UV or VUV photons radiating from the high-density plasma etching technique lead to generate crystal defects.

These problems strongly degrade electrical properties of nanoscale devices. Therefore, these problems can be avoided using high-performance neutral-beam etching system. S. Samukawa and his group have invented a highly efficient neutral-beam source to realize the ultimate top-down etching for future nanoscale devices. They introduced the ultimate etching processes for future nanoscale devices from 50 nm to sub-10 nm in using our new neutral beam sources.

This letter is therefore organized as follows. Firstly, the historical roadmap of electrical doping is briefly reviewed. After that, we will review some experimental work at the molecular level as this doping process has its impact on the molecular level, too. Then, we give brief discussions on a variety of research works associated with the electrical doping process. Some of the importances of electrical doping are described in the following section. Furthermore, we describe the method of the electrical doping process. Finally, we will conclude with the brief discussion of the comparative study between conventional doping and electrical doping.

## Historical Roadmap of Electrical Doping

Although this study mostly concentrates on electrical doping at the molecular level, it is important to first review the early history of conventional doping. In the year of 1930, it was noticed that the conductivity of semiconductors was affected due to the presence of a little number of impurities [2, 22, 23]. In the year 1931, the first quantum–mechanical formalism was used for semiconducting materials [24]. The prototype of a p–n junction was successfully demonstrated by Davydov in the year of 1938 [25, 26]. This article explained the importance of minority carriers. Woodyard introduced the concept of "doping." He incorporated a small portion of phosphorus, arsenic or antimony into pure germanium. This addition of impurity increases the electrical properties of germanium [27]. Shockley proposed his historical invention, i.e., "junction transistor" in the year of 1949. This invention changes the geometry of the semiconductor industry [28]. Though the invention of bipolar junction made a tsunami to the evolution in the semiconductor industry, it had several problems too related to transistors. For example, two p–n layers should be junction together back to back within a thin space. This problem was removed after the invention of "grown junction transistor" at Bell laboratory in the year 1950 using a double-doping method [29, 30]. In the case of the "double-doping" process, a pinch of gallium was added into the molten n-type germanium, which transformed germanium into p-type. Afterward, a pinch of antimony was included to it which transforms it to p-type back to n-type [31]. Two types of dopants were added back to back in this process. There is another kind of doping that was evolved in the early 1950s, which is known as

Dey *et al. Nanoscale Res Lett*    (2021) 16:20

Page 3 of 16

"co-doping." The p and n junctions are considered as "co-doping" of a semiconductor. The doping at the molecular level is also an important part of electrical doping. In the year of 1998, Rudaz proposed a method to maximize the effect of electrical doping by reducing material cracking for III–V semiconductors [4]. In the year of 2002, Zhou et al. demonstrated vacuum-deposited transparent organic light-emitting diode which is also a low-voltage device by using the electrical doping process. Electrical doping plays a crucial role to improve the performance of organic devices. Electrically doped carrier injection takes place for organic LEDs (OLEDs). The transport layers show low driving voltages, which is generally due to the radical anions, cations and ohmic contacts at the end of the electrode interfaces. Ultra-low-voltage OLEDs are vacuum deposited with 2.6 V for 100 cd/m$^2$ in p–i–n structure. Therefore, an intrinsic emission is sandwiched between p- and n-type wide bandgap transport layer. The activities related to electrical doping in organic molecular films are emphasized in a few studies [32–42].

This is one of the procedures to avoid the ionic bombardment process in the atomic-scale device designing approach. Gao and Kahn [43] have demonstrated this process onto the molecular thin films. These compounds for example poly-carbonate polymer with tris(4-bromophenyl)aminium hexachloroantimonate (TBAHA) 4,4′,4″-tris(3-methylphenylphenylamino)-triphenylamine (m-MTDATA) hole transport layer p doped with F4-TCNQ are used to successfully fabricate various OLEDs compound device layer [45, 46]. This process has also been used in organic photovoltaic cell (OPVC). This process has also been used for tuning at the molecular level and also for improving the device efficiency enhancement by carrier injection. Molecular film conductivity increases to a large extent for n- and p-type doping by using this process. This doping process is extensively used for ohmic contacts on inorganic semiconductors [43–46]. Nowadays, organic LEDs hold effective footage in the field of molecular nanotechnology. In III–V semiconductor, using this doping process n-type contacts and insertion of n-type external molecules can be made possible. Electrical doping also helps to make possible the phenomenon like electrical resistance, carrier insertion, carrier recombination into the molecular interfacing layer. Organic photovoltaic cell (OPVC) is one of the most relevant applications of the electrical doping phenomenon. In the process of level alignment for OPVC, this process acts on the conductivity of these cells. Charge carrier insertion is eventually increased by this method. In the case of meta-organic interfaces, this method begins and brings to the arrangement of a depletion layer through which quantum tunneling transmission can take place. This is one of the efficient processes

which can be effectively used for organic and inorganic contact fabrication. This process also helps to shift the charge neutrality levels for molecular thin films. In addition to this, approximately 0.1 to 1% of foreign molecules can be included using this method to the molecular interfaces. This amount of doping concentration is a large number for the conventional doping method. This level of doping concentration helps to generate de-generates semiconductors. This high doping concentration helps to prevent the subsequent formation of doing-induced bands [34, 43–46].

## Electrical Doping Process and Its Importance

The main and foremost technique opted for the electrical doping method is to control the Fermi level using this process. Therefore, this technique is highly popular among inorganic and organic semiconductors for the past few decades. Electrical doping in recent years has attracted special attention in the field of bioinspired nanotechnology. Electrical doping is the process of electronic charge insertion or acceptance of them to molecular films. The key feature of this process is that the conventional n and p doping cannot be constrained to accomplish the bipolarity. The conventional ionization process is not applied for this type of electrical doping process [43–46]. The electrical doping procedure has been introduced to avoid ionic bombardment, which is generally not possible for nanoscale device modeling.

This method of doping was determined mainly in two steps:

> The first step is involved with a single electron transfer from donor to an acceptor (into molecules).
> Secondly, it is associated with the method of dissociation of ground state integer charge-transfer complex.

Thus, it is confirmed that electrical doping is nothing but to shift of the Fermi level either toward the highest occupied (valence band) molecular level or lowest unoccupied (conduction band) molecular state. If the free carrier is $\rho$, $N_A^-$ is ionized dopant density, $N_A$ is the neutral dopant concentration, then the free carrier density is to be formulated as in Eq. (1). In this equation, $E_A$ and $E_F$ are the acceptor and Fermi-level energies and $K_B$ is the Boltzmann constant at absolute temperature $T$ [124].

$$\rho = N_A^- = \frac{N_A}{1 + \exp\left(\frac{E_A - E_F}{K_B T}\right)} \tag{1}$$

This doping technique has been carried out using two-probe design techniques in Atomistix Tool Kit-Virtual Nano Lab (ATK-VNL). The number of bioinspired

Dey *et al. Nanoscale Res Lett*    (2021) 16:20

Page 4 of 16

atomistic devices lies at the heart of nanotechnology. These devices operate at ultra-high THz frequency. The frequency that is calculated for these device is around THz. For example in a article, where transport characteristics for GaAs-Adenine-GaAs semiconductor tunnel junction is illustrated. In that article the operating frequency is reported about 25THz [125].

Doping is an intentional induction of external impurities into a pure semiconductor material for the reason of enhanced electrical performances. Importance of electrical doping process can be described as follows.

This electrical doping procedure is different from the conventional doping process. In the case of the conventional doping process, the semiconductor material is doped with extrinsic dopants or impurity. This process is the high-temperature process. There is a chance of breakage of bonds that may happen during this high-temperature doping process. The ionization method is also adopted to implement this doping method. On the other hand, the electrical doping process is not related to impurities at all. As in this procedure, opposite potential charges are induced at the two ends of the device. Therefore, it will generate a potential drop in the central molecular region of the nanodevice. This method is quite helpful for nanodevice designing because the ionization method may generate structural deformation for the nanomaterials. In the case of conventional doping, several problems may arise. Some of the major problems are listed in Table 1. Differentiation between conventional and electrical doping is framed in Table 1, and it also helps to understand how electrical doping is important for nanoscale device fabrication.

This Table 1 shows why electrical doping is important for molecular level. This doping avoids the heat generation, interatomic or intermolecular reaction along with it is compatible for any kind of nanoscale device designing procedure.

In this article, electrical doping process is mainly highlighted. This doping method is useful for nanoscale device fabrication mainly molecular thin film preparation. In this method insertion of charge carriers takes place at the two ends of the molecular device. This process is also depicted in Fig. 1. This diagram represents the
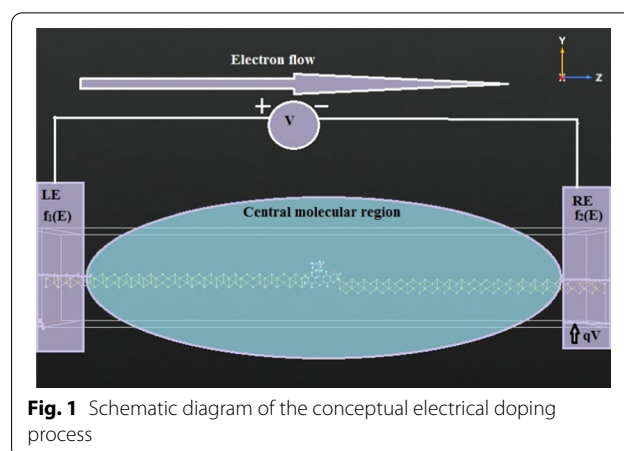


**Fig. 1** Schematic diagram of the conceptual electrical doping process

simple electrical doping method. This figure also shows how potential drop has been created due to the insertion of two equal but opposite charge carrier insertion at the two terminals of electrodes. These electrodes are the important part of molecular device. The charge insertion can be done through these electrodes. This equal and opposite charge creates a potential drop within the central molecular region. This potential drop acts as the driving force of charge conduction between two electrodes, i.e., through the central molecular part. This is the actual process of electrical doping. Though this process is nowadays used in analytical or theoretical modeling of nanoscale devices mainly, also it is useful for organic and inorganic molecular thin film preparation.

Figure 1 shows how electron or charge carrier flows from one electrode to another direction due to the potential drop that has been imposed due to variation of bias at the two terminals of electrodes.

## Electrical Doping at the Molecular Level

Recently researchers are interested for controlled doping procedure. Therefore, this electrical doping procedure helps to introduce controlled doping for inorganic semiconductors. Thus, it is also helpful to tune electrical properties of these semiconductors by introducing electrical doping. This doping phenomenon helps to tune optical gap of semiconductors with their chemical

**Table 1  Difference between conventional doping and electrical doping**

| Conventional doping | Electrical doping |
| --- | --- |
| A little amount of interaction is observed between dopant and host atom | There is no chance of interaction between host and dopant atoms |
| Mismatching of compatibility between foreign atoms and host atoms | No probability of compatibility mismatching as it depends on bias voltage |
| The exothermic reaction may take place | There is no chance of heat generation. Because heat may destroy molecular thin films |
| The intermolecular reaction may be observed during this process | No intermolecular reaction takes place |

Dey *et al. Nanoscale Res Lett*　　(2021) 16:20

Page 5 of 16

variation. This doping procedure is also a low-cost process and useful for flexible substrates.

The electrical doping procedure is the method by which a potential difference has been created between the two ends of the nanodevice. In this theoretical work [47–52] we have arranged this by providing different polarity but same-valued voltage at the two ends of the nanodevice via two-probe electrodes. The schematic diagram for this theoretical process is shown in Fig. 2.

This theoretical approach is involved to create highly doped positive (p+) and negative (n+) regions, which are important to design nanosemiconductor devices for both organic and inorganic materials.

Using this procedure charge carriers are to be injected into the molecular interfaces. Electrical doping is a controlled process for organic molecules rather than inorganic thin films. Therefore, conventional p and n dopants are not mandatory for insertion. Eventually, electrical doping increases carrier injection and decreases drive voltage which leads to a rise in device efficacy. Thus, electrical doping method solely depends on the injection of either electronic transmission or electron reception to the host molecule.
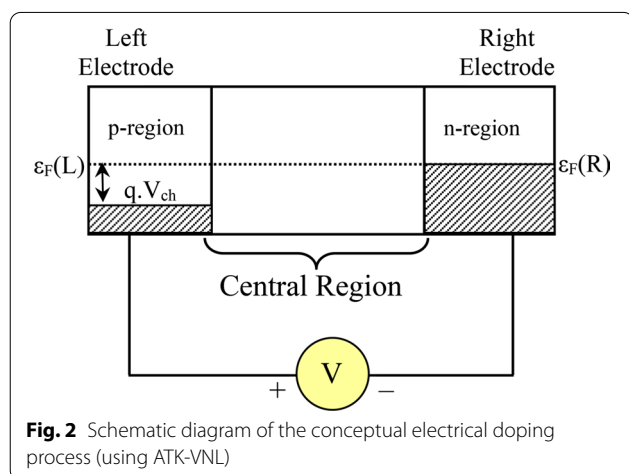
The heterojunction chain is made with adenine and thymine biomolecules used to sense several gases when the chain passed through the nanopore of a GaAs nanosheet [47]. In that case, also the electrical doping is induced at the two parts of this nanosheet. Due to the effective inductance, this biomolecular chain shows its ability to sense the adsorbed foreign gas molecules [47]. In the case of nanodevice design is also dealt with adsorption of molecules. For example, adsorption of volatile molecules at 32 °C temperature into ZnO nanowire is investigated [53]. Using DFT and NEGF formalisms-based first-principle approach, nano-FET can be designed using various structural modifications. Various properties of these

nano-FETs' are also observed, for example, scalability assessment, highest occupied molecular orbital–lowest unoccupied molecular orbital (HOMO–LUMO) gaps, maximum obtainable current, RF performance, linearity investigation [54–61]. Conjugated co-oligomers-based molecular diode can be designed using DFT- and NEGF-based formalisms. The co-oligomers are connected with two electrodes and form a molecular diode. The energy gap, current–voltage (I–V) characteristics, spatial orientations are analyzed for this diode [62]. The first-principle approach is applied to the geometrically optimized nanostructures of seven different junctions which are derived from carbon nanotube (CNT) using different linkers [63]. Various types of diodes can be implemented using DFT and NEGF formulas-based first-principle approach. For example, Schottky diode, single molecular diode, spin current diode, bipolar spin diode, di-block molecular diode, backward diode characteristics are therefore implemented using this approach [64–68].

## Molecular-Level Research Works Based on Electrical Doping

Electrical doping at molecular level plays an important role in nanoelectronics. Researchers are highly interested to introduce this doping procedure at nanoscale device designing procedure. The effect of this doping helps to interface between different molecular level of alignment. This process is not only helpful to study organic heterojunction molecular level but also acceptable for inorganic materials. This doping helps for the interface formation with the help of dipole and equivalent move in comparative position of molecular interface. Thus, this process of electrical doping is acceptable for molecular interface alignment.

Miniaturization of conventional electronic devices is the most emerging research area nowadays. There are several approaches which lead to motivate researchers to investigate and study the nature of nanoscale devices. One of the most important approaches is to design and simulate analytical nanostructures. Many significant devices can be designed using this simulation procedure and analyze the obtained results [47, 55, 56]. According to the result, the researchers can modify the various simulation parameters as well as the different aspects of the nanoscale analytical model. Among these simulation methods, the first-principle approach is the most effective and popular process. Modernization of electronic devices encourages researchers to innovate conventional devices in a modified version. For example, traditional semiconductor devices can be designed using biomolecules. In the case of biomolecules generally, nucleobases such as adenine, thymine, guanine and cytosine have been considered which are known as the basic building

**Fig. 2** Schematic diagram of the conceptual electrical doping process (using ATK-VNL)

Dey *et al. Nanoscale Res Lett* (2021) 16:20

Page 6 of 16

blocks of DNA [47, 55]. It is very common to construct conventional inorganic semiconductor devices in the field of nanotechnology. However, it is hard to construct organic electronic devices mainly using biomolecules. These semiconductors are characterized depending upon the doping properties. If the semiconductor does not have any impurity doping, then it is called intrinsic or pure semiconductor. On the other hand, if the semiconductor is doped with foreign atoms or molecules, then it is known as an extrinsic or impure semiconductor [55–60].

Nowadays, nanoscale device designing is a challenging aspect for researchers. Diode, transistor, logic gates have already been implemented at the molecular level. There is another scope for researchers to implement nano-biosemiconductor devices at the molecular level. Some of these biomolecular devices have already been introduced in the arena of biomedicine. The theoretical design of these nanodevices has been implemented using the Atomistix-Tool Kit and Virtual Nano Laboratory (ATK-VNL)-based Quantumwise software simulator version 13.8.0 [69–76]. Even Quantum Cellular Automata (QCA) logic can be theoretically implemented using DFT and NEGF-based first-principle approach [77]. Various logic gates can be made possible to design using biomolecules, and the results obtained from these theoretical implications have also validated using Multi-Sim or SPICE or other simulators [70]. The electrical doping process is the key feature that is introduced to obtain optimum current. Tunnel current through the molecular channel is affected by various factors like back-scattering effect, etc. By implementing this doping process, we can avoid the problems related to the conventional doping process. The dipole combination model for Schottky barrier tuning is also suggested at the metal–semiconductor interface at the molecular level [78]. The first-principle approach is also applicable for magnetic tunnel junction, and their quantum electronic properties have been analyzed [79]. To calculate leakage current through $SiO_2$ and $SiO_xN_y$-based MOSFET, researchers used DFT- and NEGF-based first-principle approach [80]. This ab-initio modeling is applied for modeling of Schottky barrier height tuning using the yttrium and nickel silicide atomic-scale interface [81]. Direct band to band tunneling in reverse-biased MOS2 p–n junction nanoribbon can be described using DFT and NEGF [82]. The effect of incorporation of opposite polarities dopant atoms into the nanowire exhibits electrical properties like Zener diode [83]. The dual-spin filtering effect can be seen in the half-metallic yttrium nitrite $YN_2$ [84]. Investigation of heterostructure biomolecular FET can be observed using this electrical doping technique. The quantum ballistic transport can be observed using this electrical

doping phenomenon at the molecular level [85]. Using this theoretical approach electrically doped biomolecular switch is designed when using single-wall carbon nanotube (SWCNT) as electrodes [86]. NEGF formalisms help to design graphene-based anti-dot resonant tunnel diode [87]. Atomistic characteristics of two-dimensional silicon p–n junctions have been demonstrated using the first-principle approach [88]. Diode and transistors are the basic building blocks of any electronic circuitry. Logic gates can also be implemented using diodes and transistors. Therefore, any logic can be implemented using first-principle formalisms.

In the recent trend of nanotechnology, researchers have interested to design and characterize the various electromechanical features of bioinspired and semiconductor devices at the atomic scale. These bioinspired devices are highly biocompatible and create a bridge between the semiconducting area and the bi-molecular research arena. CMOS technology has been already saturated. Therefore, the aim of the researchers is to replace and create a bridge between them. Several proposals have already been raised by the researchers to join the CMOS technology with bioinspired technology like DNA or any other biomolecules. The important parts of the DNA are adenine, thymine, cytosine and guanine nitrogen bases. These nitrogen bases have made composites with ribose sugar and phosphate groups to form oligonucleotide. This oligonucleotide has phosphate groups as the backbone. Correlations for dynamic signals have been enhanced for the identification of biomolecules and DNA [89]. DNA translocation, electronic transmission and semiempirical modeling through graphene nanopore can also be made possible theoretically using DFT and NEGF [90–93]. DNA analysis can also be made possible with graphene electrodes using semiempirical modeling [94]. Recognizing of nucleic acid base pairs using transverse transport properties has also been made possible [95]. Conductance through shot DNA has also been proposed by the group of researchers [96]. Electronic enhancement by doping procedure to the DNA base pairs has also been incorporated to enhance the conductivity [97]. The electronic promotion has also been possible by the double-proton transfer process [98]. Recognition of nucleotides by the cross-tunneling method has also been possible using the first-principle approach [99]. Structural factors control the conductivity of DNA, and this has also been discussed in [100]. The nanoscale devices exhibit an enormous quantum transport phenomenon for different types of nanoscale device modeling [56, 58, 59, 101–107]. These devices include FETs, diodes and optical switches [60, 68, 108–116]. This proposed work is one approach to make a bridge between the biomolecules with III–V semiconductor technology. The heterostructure of

biomolecules and III–V nanocrystalline materials can also be designed using the first-principle theoretical approach. Furthermore, electrical and optical properties of nitrogen and gold co-doped graphene are investigated using first-principle formalisms. First-principle formalism is used to find out the change of quantum–mechanical characteristics and investigation of various electronic or optical properties of the organic as well as inorganic molecules. Investigation can also be done for vacancy-defected graphene and Mn-doped graphene toward the $H_2S$ absorption. Ferromagnetism investigation using the first-principle approach for transition-metal doped AlN monolayer is also an emerging trend. Doping effect is investigated for monolayer $MoS_2$ using DFT for visible light is an important topic of discussion. A study of change of electronic properties was demonstrated for Eu-doped phosphorene based on the first-principle approach. Electromechanical quantum transport features are available for these devices [117–121].

In the year of 1987, Destefanis proposed the electrical doping of HgCdTe using ion implantation and heat treatment method. To increase a large number of pixels into the focal plane array devices, infrared photovoltaic detectors were required. The use of ion implanting HgCdTe was increasing this interest of manufacturers. In this type of manufacturing of photovoltaic infrared detectors, the electrical doping process was introduced. It was revealed that the effect of electrical doping into HgCdTe appeared significantly as the intrinsic properties of diodes were directly related to it [122]. Electrical was also proposed for enhancement of plasmonic absorption on Au-PbS core–shell nanocrystals. This method of doping was implemented using the intra-particle charge transfer method. In this experiment, colloidal nanocrystals were used to be the basic building blocks for solar cells, photo-detectors, etc. In this approach, researchers investigated the electronic properties of colloidal nanocrystalline materials and they also proposed a novel approach to electrical doping to these nanocrystalline solids using intra-particle charge transfer method [123]. The process flow for this simulation work is shown in Fig. 3.

## Simulation Methods of Electrical Doping

The analytical design of these molecular devices requires constant innovation and improvement in the field of material science. Density functional theory (DFT) and non-equilibrium Green's function (NEGF) are the two key formalisms behind the analytics for the modeling of these nanoscale devices. The first-principle approach combines these two formalisms to describe theoretically these types of nanodimension devices. Extended Hückel theory (EHT) is another key factor

to accelerate the design procedure of these atomistic devices [126, 127]. These theoretical modeling procedures help to prevent various problems regarding the nanoscale design like hazards during doping of foreign particles, generation of THz operating frequency, etc. Another aim of this nanoscale design procedure is to operate the device by keeping the electronic temperature at 300 K, i.e., room temperature. III–V semiconductors are optically sound semiconductor material that can be used for the design of various electronic devices. After silicon technology, III–V semiconductor technology is one of the emerging and most desirable areas to be fit in the nanoscale semiconductor technology. Biomolecules (like adenine, thymine, guanine and cytosine) have been introduced to form different nanoscale electronic devices. These biomolecules also exhibit their optical exposure whenever they are simulated at near-UV region (mid-UV-B). In this proposed work the electronic characterization has been made for the simulated nanoscale devices using the first-principle approach. This semiempirical modeling is carried out using EHT for obtaining faster simulation. We aim to design and characterize the III–V materials along with biomolecules using DFT- and NEGF-based first-principle formalisms. This semiempirical design of this bioinspired nanodevices has been carried out using the Quantumwise software simulation package.

To include electrical doping into the molecular devices, the same but opposite charge is to be provided to the two ends of the molecular interface. The electrical doping concentration is calculated using the following procedure:

Let us assume the electrodes are about 1 nm long and with 0.5 nm × 0.5 nm cross-sectional area. For simplification of calculation, we have taken those values. In the script editor, we have located the section for the electrodes calculator and assigned the charge = + 0.01 and − 0.01. For this theoretical study, the Atomistic Tool Kit-Virtual Nano-laboratory (ATK-VNL) software package has been used. This software uses density functional theory (DFT) and non-equilibrium Green's function (NEGF)-based first-principle approach. This value is being calculated using the following formula:
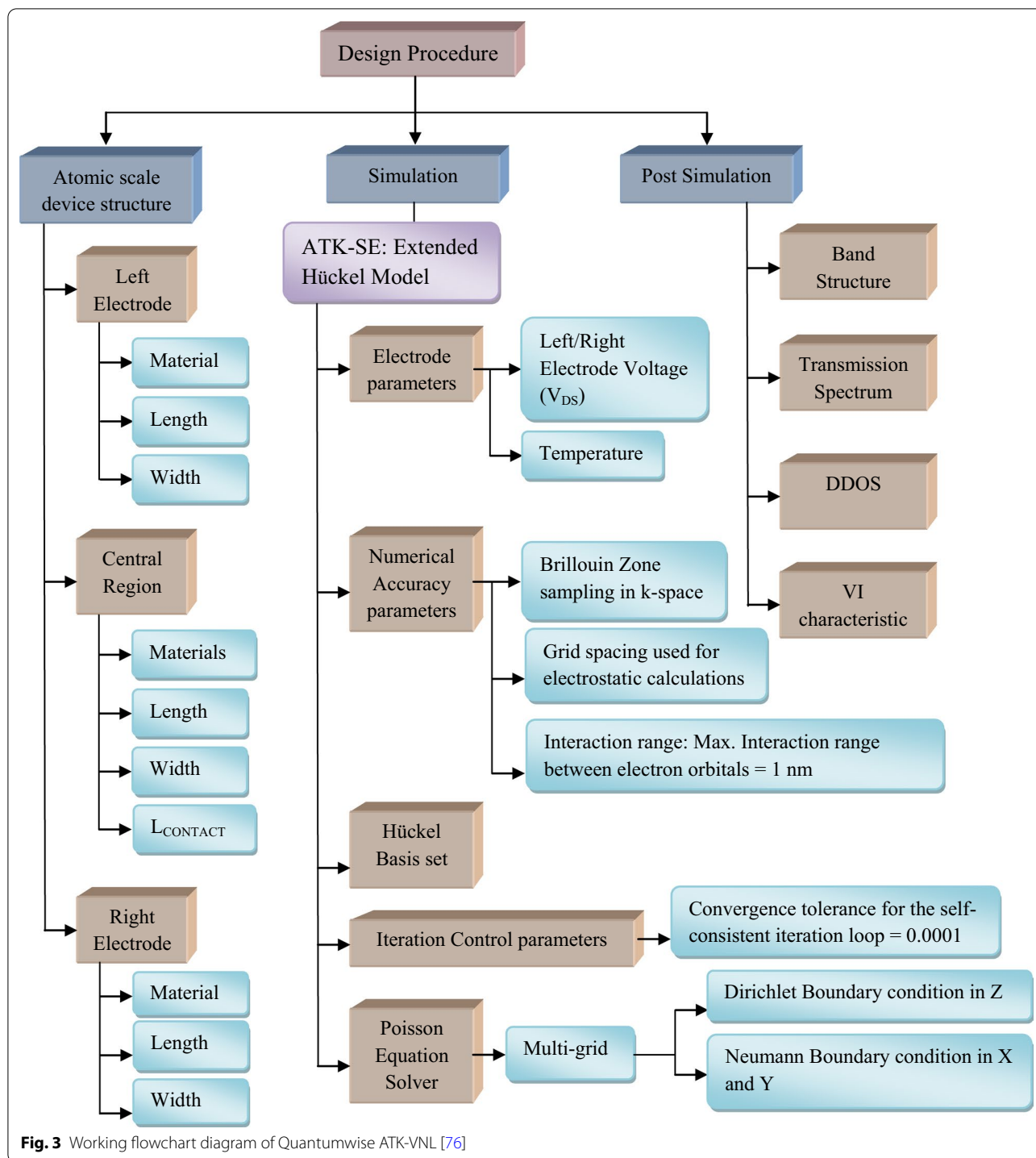
Effective doping concentration = doping/volume [1, 70, 71]

Assume, doping charge = ± x V

Assume that, volume = length $(a)$ × width $(b)$ × height $(c)$ = $a \times b \times c$

Volume = $(a \times 10^{-7}) \times (b \times 10^{-7}) \times (c \times 10^{-7})$ cm$^{-3}$ = $abc \times 10^{-21}$/cm$^3$

Effective doping = $\frac{x}{abc \times 10^{-21}}$ = $abc \times 10^{21}$/cm$^3$ [as we have consider the dimension in nm unit]

**Fig. 3** Working flowchart diagram of Quantumwise ATK-VNL [76]

The volumes of the electrodes remain constant so from Fig. 4, it can be observed that the doping concentration is directly proportional to the applied bias voltage. This is another reason that we have kept constant the electrode's size. The little change in electrodes' size leads to a large change in electrical doping concentration. So by changing the little amount of bias voltage we can be able to generate very high electrical doping into the system using the first-principle approach.

The electrical doping in this case totally depends on two parameters mainly. They are (1) effective doping charge (charge applied at the two ends of the electrodes)

**Fig. 4** Dependence of effective electrical doping on an applied bias voltage
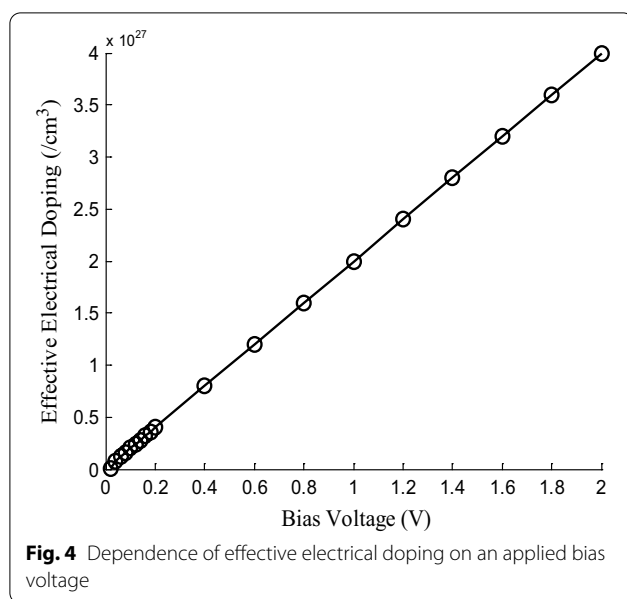
and (2) volume of the nanoscale device. Therefore, the formula of calculating electrical doping is mentioned as doping/volume, so if the length, height or breadth or anyone of the parameter is changed, then the doping concentration is definitely changed. For this type of device structure, volume is a function of length, height, width [70].

Both the temperature and thickness affect the performance of these nanoscale devices. Self-heating effect along with thermal noise generated heat also makes changes in quantum-ballistic transport phenomenon of these devices at this low dimension. Therefore, temperature plays an important role in the device performance. On the other hand, as thickness is related to the volume of the device and effective doping is directly related to volume, thickness also affects device performance. If thickness is changed, then accordingly volume changes which result in changes of doping concentration. Doping concentration is related directly to device performance like channel conductivity, current–voltage characteristics, etc., for these nanoscale devices. Therefore, doping is changed due to thickness changed that will definitely change device performance [70].
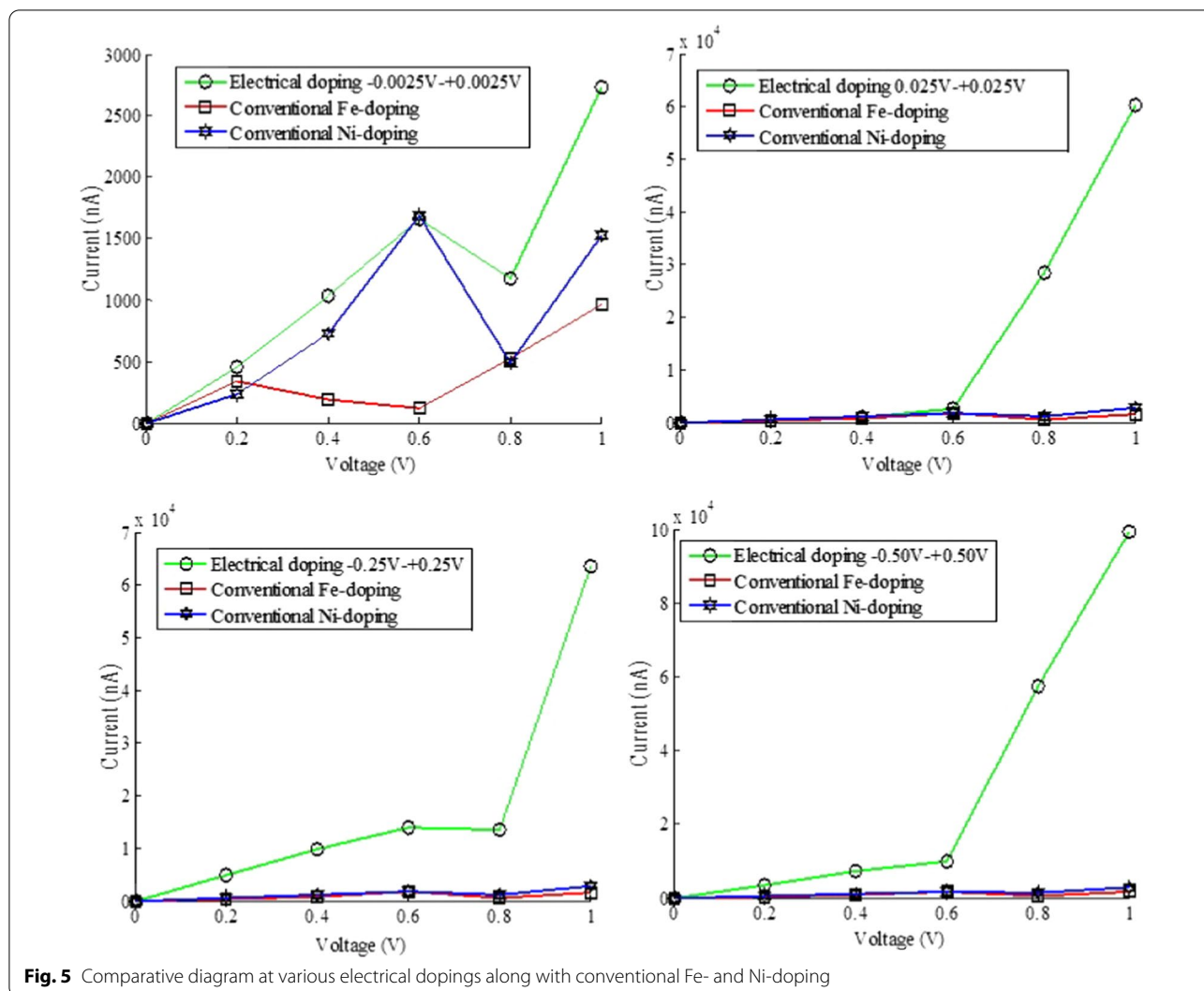
## Evolution of Electrical Doping

Doping means the addition of explicit impurity atoms to the semiconductor. Doping is the intentional addition of atoms to the intrinsic semiconductor to modulate the electrical properties of intrinsic semiconductors. The electrodes sizes are inserted within the script editor, where we assigned the length of the electrode as 1 nm and cross section 0.5 nm × 0.5 nm. Thus, the nominal

charge, i.e., ±0.01, is set for the two electrodes. This script is processed through the job manager, and the calculated doping value for the electrodes is obtained. For this calculation we pursue the following steps:

- Open the New Calculator and select "ATK-SE: Extended Hückel (Device)."
- Uncheck "No SCF iteration."
- Keep mesh cutoff to 10 Hartree.
- Under "Poisson Solver" set the "Neumann" boundary conditions along A(X) and B(Y) directions.

Figure 5 shows the consolidated form of the comparative study between electrical doping and conventional doping process (using Fe and Ni). This analytical experiment is observed for the thymine nanotube structure which is an example of electrical doping [70]. Fe and Ni atoms are chosen to dope the thymine nanotube, and on the other hand, the molecule is electrically doped [70]. All these results show that amount of electrical doping is much more when compared with conventional doping for little amount of applied bias. Some example works of electrical doping along with its some advantages over conventional doping are discussed in Table 2. It gives a comparative study of electrically doped devices with the existing device modeling which follows the conventional doping method. There are several types of doping, and dopants are available, for example, conventional doping (by adding impurity), electrical doping, co-doping. Generally, two types of dopants are available for conventional doping process, p-type dopants and n-type dopants. They are often called as acceptor and donor impurity atoms. These external impurities are added to the semiconducting materials to enhance their electrical properties mainly conductivity. In the case of the electrical doping process, mainly for analytical modeling using the ATK-VNL approach, we do not proceed with the addition of foreign atoms. Instead of these explicit atom doping, we focus on the change of potential difference at the two ends of the device (mainly at the ends of electrodes). The doping of a semiconductor along with another substance is known as co-doping. For example, when Co and N both are added to $MoO_2$ nanowires, it will increase the electronic performance of this nanowire [128–130]. Various properties like electronic, optical and morphological characteristics of p-doped polyfuran (PF) molecular thin films were investigated by the researchers using a wide range of doping ratios using the electrical doping method. When the doping concentration is ≤ 2%, then it increased the short-circuit current of this PF-based photovoltaic device significantly [44].

If we take a close look at the doping concentration from Fig. 6, we can observe that before the year 2000, doping

Dey *et al. Nanoscale Res Lett*    (2021) 16:20

Page 10 of 16



**Fig. 5** Comparative diagram at various electrical dopings along with conventional Fe- and Ni-doping

concentration was high, but after that, it becomes lower. Therefore, it can be emphasized that though the device performance has been enhanced, doping concentration is reducing very fast [124, 128, 134–136].

The optical and electrical doping process was also introduced into the silicon with holmium in the year 1999. Intermolecular hybridization state is also governed by the electrical doping process. It was established that for organic semiconductors, molecular electrical doping was found to be at odds when other methods were proved in this field, for example, the formation of polaron. Therefore, the main objective of this study is to propose a polaron-derived state with decreased ionization energy using ultraviolet photo-electrospectroscopy [134]. The electrical doping profile in ferroelectric film capacitors was investigated by the group of researchers using capacitance–voltage measurement. In this experimental study, profiling effect of

electrical doping concentration in ferroelectrics was investigated using the following effects of

A field and spatially dependent permittivity.
Domain switching analysis of Schottky profiling [135].

From Fig. 7, we can observe the operating temperature for this type of doping-dependent device operation. Though the graph is a little bit complex, it does not obey any specified rule. Therefore, we can conclude it like that temperature requirement is solely depending on the type of materials that are used for this operation.

A new model was proposed for the dissociation of carbon atoms at the copper/silica molecular thin layer interface using catalytically hydrogenated graphene meshes using a semipermanent electrical doping

**Table 2** Comparative study of conventional doping with electrical doping

| Various doped materials features | Conventional doping | | | | Electrical doping | | | |
|---|---|---|---|---|---|---|---|---|
| | Chlorine-doped WS$_2$-metal interface [131] | Co-doped ZnO structures joining the Al electrode [132] | Doped armchair graphene nanoribbons [133] | Carbon nanotubes with boron/nitrogen co-doping [52] | Electrically doped pin FET from adenine-based single-wall nanotube [55] | Electrically doped gated diode from single-wall nanotube-like structure [70] | GaAs pin nanodiode [75] | Electrically doped nanobiopin FET [76] |
| Maximum current achieved | Data not given | − 4862 nA | $6.16 \times 10^{-6}$ A | Data not given | 15.9 μA | 99.3 μA | 1.16 μA | 35.96 nA |
| Composite central region length | 5 × 5 WS2 super-cell (inorganic, metal interface) | Inorganic (ZnO) | Organic (graphene nanoribbon) | Organic (carbon nanotube) | Biomolecular, 3.35 nm | Biomolecular, 3.75 nm | Inorganic (GaAs), electrode is 1 nm with a cross section of 0.5 nm × 0.5 nm | Biomolecular, 6.24 nm |
| Operating temperature | Room temperature | Room temperature | Room temperature | Room temperature | 300 K | 300 K | 300 K | 300 K |
| Force tolerance | 0.001 eV/Å | 0.05 eV/Å | NM | 0.01 eV/°A | 0.01 eV/Å | 0.01 eV/Å | 0.05 eV/Å | 0.05 eV/Å |
| Applied bias (V) | – | − 1 to +1 | Low | – | 0.02 | 0.0025–0.5 | ±0.01 | ±0.01 |
| Doping concentration | 2% of total sulfur atoms | 2.5% of total Zn atoms | Satisfactory | B/N pairs: 5% and 10%, respectively | $3.05 \times 10^{18}$/cm$^3$ | $5.73 \times 10^{18}$/cm$^3$ | $5.23 \times 10^{19}$/cm$^3$ | $4 \times 10^{19}$/cm$^3$ |
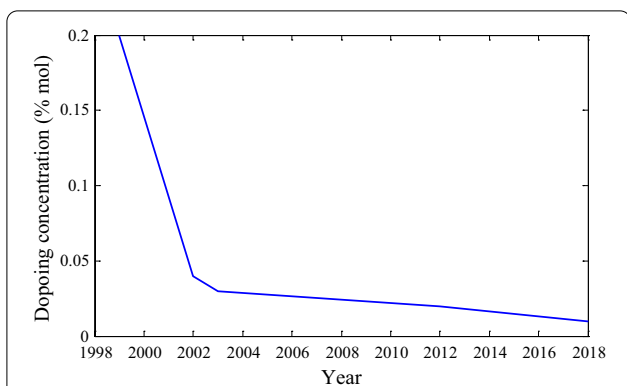
**Fig. 6** Doping concentration year-wise graph
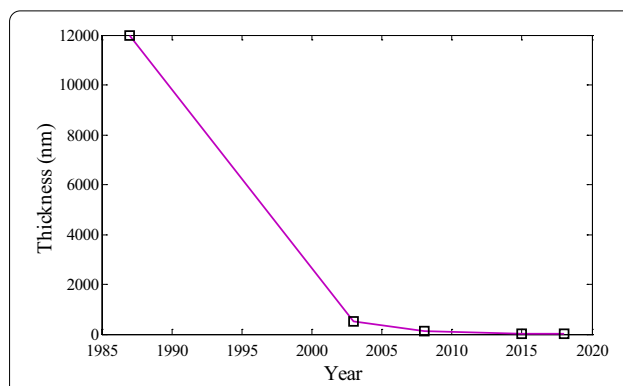


**Fig. 8** The thickness of the wafer
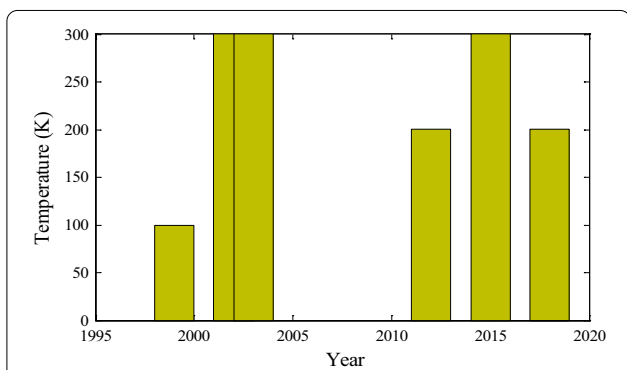


**Fig. 7** Temperature for doping
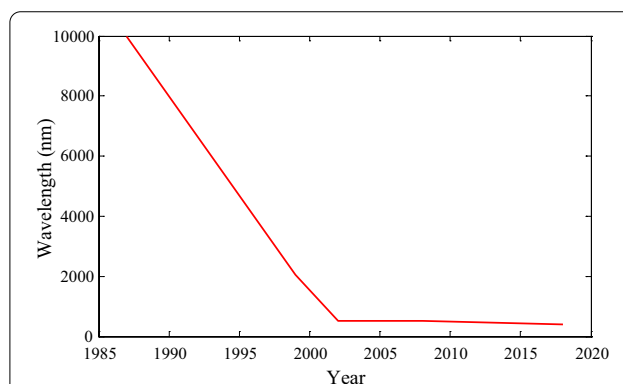


**Fig. 9** The wavelength of the devices reduces

method. This process enables stable electronic doping through C–N bonds. Furthermore, the effect of trap states on the electrical doping for organic semiconductors was also investigated. The direct charge transfer process from the trap state of the host molecules to the dopant molecules raised the electrical effect for organic semiconductors. This type of doping process enhances conductivity. Therefore, trap density and energy are also analyzed using impedance spectroscopy [136].

It is observed clearly from Fig. 8 that the thickness of the wafer layers is reducing year wise. The more the time increasing, the layer thickness reduces, and the performance of the device increases.

Electrically doped and undoped poly(9,9-dioctyl-fluorenyl-2,7-diyl) (PFO) along with tetrafluorotetracyanoquinodimethane films were composed using photoelectron spectroscopy method and also investigated their current–voltage characteristics. Thus, it can be observed that the depletion region was created for the PFO interface. Therefore, the current was increased subsequently [137, 138]. For high-temperature gas sensors, this method of doping plays an important role. The conductivity and gas sensitivity of $Ga_2O_3$ thin films

was investigated. It was observed that this doping concentration influenced the surface sensitivity [138].

From Fig. 9, it is observed that the cutoff wavelength of the devices reduces sharply within a few decades. Hence, device performance enhanced significantly. Table 3 gives a close look at different characteristics of the devices which follow either electrical doping or conventional doping procedure.

In this survey, we have reviewed the works which were already established using the electrical doping process. In our works, we used the electrical doping process using the Quantumwise software simulation package in the ATK-VNL atmosphere. The version of this software is 13.8.0. This software simulation is based on first-principle formalisms which is again strongly supported by DFT and NEGF formalisms. Quantumwise is a compact set of atomic-scale modeling tools. These tools were developed in the year of 2003 by some software professionals along with academicians. These ATK-VNL simulations engines help us to calculate the electronic structure as well as to formulate

**Table 3** Several properties of the devices with conventional doping and electrical doping approaches at a glance

| Article with Ref. no. features | Electrical doping approach | | | Conventional doping approach | | |
|---|---|---|---|---|---|---|
| | Yu et al. [44] | Lee et al. [123] | Tietze et al. [124] | Ling et al. [48] | An et al. [49] | Liu et al. [97] |
| Device | Polyfuran-based photo-voltaic cells | Au-PbS core–shell nanocrystals | OLEDs | Triangular graph-eme with B/N doped | Graphene nanorib-bon | Copper-modified DNA |
| Conductivity | High | 1 S/cm | $> 10^{-2}$ S/cm | – | – | Enhanced |
| Driving voltage | Low open-circuit voltage 0.2–0.4 V | − 40 to + 40 V | − 2.0 < V < 0.3 | − 2.2 to 2.2 | – | − 0.6 to + 0.6 V |
| Doping | Dopant concentra-tion ≤ 2% | High doping density | 0.1 mol% | B/N doped | B/N doped | Cu doped |
| Procedure | Atomic force micros-copy | Intra-particle charge transfer (plas-monic enhance-ment) | Ground state integer charge transfer | NEGF + DFT | DFT + NEGF | DFT + NEGF |
| Constrain | Enhanced work function at high dopant concen-tration cannot be explained by integer charge transfer | The amount of charge transferred between Au and PbS depends on the core size and shell thickness which still has to be determined | Electrical doping is not sufficient to fill the deep traps | Intra-molecular weak interaction effect on rectify-ing property | Theoretical approach | Theoretical approach |

intercorrelations of atomic orbitals. This platform helps us to introduce electrical doping into the molecular level.

## Conclusion

This report illustrates briefly a comparison between conventional doping and electrical doping process. Though the electrical doping process is not so newer process, the implementation of this process with the help of DFT- and NEGF-based first-principle approach gives a new twist to this phenomenon. Therefore, electrical doping is to be implemented in many molecular modeling approaches to bring a new era in nanoelectronics. This study takes a close look at the electrical doping phenomenon such as why it is important, how it works for the molecular modeling approach, calculation of electrical doping concentration, etc. Hence, we provide a comparative study between electrical doping and conventional doping process for acepromazine molecule. To conclude it is emphasized that in future this is one of the approaches which will prove itself in the field of nanodevice modeling.

## Abbreviations

DFT: Density functional theory; NEGF: Non-equilibrium Greens' function; OPVC: Organic photovoltaic cell; ATK-VNL: Atomistix Tool Kit-Virtual Nano-Laboratory; HOMO–LUMO: Highest occupied molecular orbital–lowest unoccupied molecular orbital; CNT: Carbon nanotube; I–V: Current–voltage; QCA: Quantum cellular automata; YN$_2$: Yttrium nitrite; ATK-SE: Atomistix Tool Kit-Semi-empirical.

## Author details
[1] Department of Electronics and Communication Engineering, B. P. Poddar Institute of Management and Technology, 137, V. I. P Road, Kolkata, West Bengal 700 052, India. [2] Department of Computer Science and Engineering, Maulana Abul Kalam Azad University of Technology, NH-12(Old NH-34), Haringhata, Post Office – Simhat, P.S. – Haringhata, Pin – 741249, Kolkata, West Bengal 700 064, India. [3] Department of Physics, University of Western Australia, M013, 35 Stirling Highway, Crawley, Perth, WA 6009, Australia. [4] Institute of IR 4.0, The National University of Malaysia (UKM), 43600 Bangi, Selangor, Malaysia. [5] Department of Chemical and Process Engineering, Faculty of Engineering and Built Environment, Universiti Kebangsaan Malaysia (UKM), Bangi, Selangor, Malaysia. [6] Institute for Mathematical Research (INSPEM), Universiti Putra Malaysia (UPM), 43400 Serdang, Malaysia.

## References
1. Freysoldt C, Grabowski B, Hickel T, Neugebauer J, Kresse G, Janotti A, Van de Walle CG (2014) First principles calculations for point defects in solids. Rev Mod Phys 86(1):253
2. Zhang J, Tse K, Wong M, Zhang Y, Zhu J (2016) A brief review of co-doping. Front Phys 11(6):117405

3.  Wei S (2004) Overcoming the doping bottleneck in semiconductors. Comput Mater Sci 30(3–4):337
4.  Rudaz SL (1998) U.S. Patent No. 5,729,029. U.S. Patent and Trademark Office, Washington, DC
5.  Haruk AM, Mativetsky JM (2015) Supramolecular approaches to nanoscale morphological control in organic solar cells. Int J Mol Sci 16(6):13381–13406
6.  Zhong A, Hane K (2012) Growth of GaN nanowall network on Si (111) substrate by molecular beam epitaxy. Nanoscale Res Lett 7(1):1–7
7.  Hsu YC, Hung YC, Wang CY (2017) Controlling growth high uniformity indium selenide (In$_2$ Se$_3$) nanowires via the rapid thermal annealing process at low temperature. Nanoscale Res Lett 12(1):532
8.  Samukawa S (2009) Damage-free plasma etching processes for future nanoscale devices. In: 2009 IEEE 22nd international conference on micro electro mechanical systems. IEEE, pp 112–119
9.  Nozawa T, Kinoshita T, Nishizuka T, Narai A, Inoue T, Nakaue A (1995) The electron charging effects of plasma on notch profile defects. Jpn J Appl Phys 34:2107–2133
10. Kinoshita T, Hane M, McVittie JP (1996) Notching as an example of charging in uniform high density plasmas. J Vac Sci Technol B 14:560–565
11. Ootera H, Oomori T, Tsuda M, Namba K (1993) Simulation of ion trajectories near submicron-patterned surface including effects of local charging and ion drift velocity toward wafer. Jpn J Appl Phys 33:4276–4280
12. Ohtake H, Samukawa S (1995) Microloading-free Si Trench etching in pulse-time modulated ECR plasma with 600 kHz RF bias. In: Proceedings of 17th dry process symposium, Tokyo, pp 45–50
13. Okamoto T, Ide T, Sasaki A, Azuma K, Nakata Y (2004) Irradiation damage in SiO$_2$/Si system induced by photons and/or ions in photo-oxidation and plasma-oxidation. Jpn J Appl Phys 43:8002–8006
14. Yonekura K, Goto K, Matsuura M, Fujiwara N, Tsujimoto K (2005) Low-damage damascene patterning using porous inorganic low-dielectric-constant materials. Jpn J Appl Phys 44:2976–3298
15. Cheung KP, Pai CS (1995) Charging damage from plasma enhanced TEOS deposition. Electr Dev Lett 16:220–222
16. Carrere J, Oberlin J-C, Haond M (2000) Topographical dependence of charging and new phenomenon during inductively coupled plasma (ICP) CVD process. In: Proceedings of 5th international symposium on plasma process-induced damage, Santa Clara, pp 164–167
17. Dao T, Wu W (1996) Charging of underlayer at via etch causing slow down in oxide etch rate. In: Proceedings of 1st international symposium on plasma process-induced damage, Monterey, pp 54–57
18. Joshi M, McVittee JP, Sarawat K (2000) Direct experimental determination and modeling of VUV induced bulk conduction in dielectrics during plasma processing. In: Proceedings of 5th international symposium on plasma process-induced damage, Santa Clara, pp 157–160
19. Cismura C, Shohet JL, McVittee JL (2000) Plasma vacuum ultraviolet emission in a high density etcher. In: Proceedings of 5th international symposium on plasma process-induced damage, Santa Clara, pp 192–195
20. Woodworth JR, Blain MG, Jarecki RL, Hamilton TW, Aragon BP (1999) Absolute intensities of the vacuum ultraviolet spectra in a metal-etch plasma processing discharge. J Vac Sci Technol A 17:3209–3217
21. Mizutani T, Nishimatsu S (1988) Sputtering yield and radiation damage by neutral beam bombardment. J Vac Sci Technol A 6:1417–1420
22. Korotkov R, Gregie J, Wessels B (2001) Electrical properties of p-type GaN:Mg codoped with oxygen. Appl Phys Lett 78(2):222
23. Kipshidze G, Kuryatkov V, Borisov B, Kudryavtsev Y, Asomoza R, Nikishin S, Temkin H (2002) Mg and O codoping in p-type GaN and AlxGa1xN (0< x < 0.08). Appl Phys Lett 80(16):2910
24. Wilson AH (1931) The theory of electronic semi-conductors. Proc R Soc A 133(822):458
25. Morris PR (1990) A history of the world semiconductor industry. IET Digital Library
26. Davydov B (1938) The rectifying action of semiconductors. Tech Phys USSR 5:87
27. Woodyard JR (1950) Nonlinear circuit device utilizing germanium, US2530110[P]
28. Shockley W (1949) The theory of p–n junctions in semiconductors and p–n junction transistors. Bell Syst Tech J 28(3):435
29. Teal G, Sparks M, Buehler E (1951) Growth of germanium single crystals containing p–n junctions. Phys Rev 81(4):637
30. Sparks M (1953) Method of making p–n junctions, US2631356A[P]
31. Choi H (2007) The boundaries of industrial research: making transistors at RCA, 1948–1960. Technol Cult 48(4):758
32. Zhou X, Pfeiffer M, Huang JS, Blochwitz-Nimoth J, Qin DS, Werner A, Drechsel J, Maennig B, Leo K (2002) Low-voltage inverted transparent vacuum deposited organic light-emitting diodes using electrical doping. Appl Phys Lett 81(5):922–924
33. Bharathan JM, Yang Y (1998) Polymer/metal interfaces and the performance of polymer light-emitting diodes. J Appl Phys 84(6):3207–3211
34. Yamamori A, Adachi C, Koyama T, Taniguchi Y (1998) Doped organic light emitting diodes having a 650-nm-thick hole transport layer. Appl Phys Lett 72(17):2147–2149
35. Blochwitz J, Pfeiffer M, Fritz T, Leo K (1998) Low voltage organic light emitting diodes featuring doped phthalocyanine as hole transport material. Appl Phys Lett 73(6):729–731
36. Kido J, Matsumoto T (1998) Bright organic electroluminescent devices having a metal-doped electron-injecting layer. Appl Phys Lett 73(20):2866–2868
37. Ma JW, Liang Z, Jin C, Jiang XY, Zhang ZL (2009) Enhanced power efficiency for white OLED with MoO3 as hole injection layer and optimized charge balance. Solid State Commun 149(5–6):214–217
38. Zhou X, Pfeiffer M, Blochwitz J, Werner A, Nollau A, Fritz T, Leo K (2001) Very-low-operating-voltage organic light-emitting diodes using AP-doped amorphous hole injection layer. Appl Phys Lett 78(4):410–412
39. Zhou X, Blochwitz J, Pfeiffer M, Nollau A, Fritz T, Leo K (2001) Enhanced hole injection into amorphous hole-transport layers of organic light-emitting diodes using controlled p-type doping. Adv Func Mater 11(4):310–314
40. Blochwitz J, Pfeiffer M, Hofmann M, Leo K (2002) Non-polymeric OLEDs with a doped amorphous hole transport layer and operating voltages, down to 3.2 V to achieve 100 cd/m$^2$. Synth Met 127(1–3):169–173
41. Huang J, Pfeiffer M, Werner A, Blochwitz J, Leo K, Liu S (2002) Low-voltage organic electroluminescent devices using pin structures. Appl Phys Lett 80(1):139–141
42. Pfeiffer M, Beyer A, Fritz T, Leo K (1998) Controlled doping of phthalo-cyanine layers by cosublimation with acceptor molecules: a systematic Seebeck and conductivity study. Appl Phys Lett 73(22):3202–3204
43. Gao W, Kahn A (2003) Electrical doping: the impact on interfaces of π-conjugated molecular films. J Phys Condens Matter 15(38):S2757
44. Yu S, Frisch J, Opitz A, Cohen E, Bendikov M, Koch N, Salzmann I (2015) Effect of molecular electrical doping on polyfuran based photovoltaic cells. Appl Phys Lett 106(20):203301
45. Kahn A, Koch N, Gao W (2003) Electronic structure and electrical properties of interfaces between metals and π-conjugated molecular films. J Polym Sci Part B Polym Phys 41(21):2529–2548
46. Kahn A, Zhao W, Gao W, Vázquez H, Flores F (2006) Doping-induced realignment of molecular levels at organic–organic heterojunctions. Chem Phys 325(1):129–137
47. Dey D, Roy P, De D (2017) Detection of ammonia and phosphine gas using heterojunction biomolecular chain with multilayer GaAs nanopore electrode. J Nanostruct 7(1):21–31
48. Dey D, Roy P, De D, Ghosh T (2016) Molecular modeling of biomolecular hydrogen gas sensor using GaAs nanopore electrode. In: 2016 3rd international conference on devices, circuits and systems (ICDCS). IEEE, pp 184–189
49. Salzmann I, Heimel G, Oehzelt M, Winkler S, Koch N (2016) Molecular electrical doping of organic semiconductors: fundamental mechanisms and emerging dopant design rules. Acc Chem Res 49(3):370–378
50. Roy P, Dey D, De D (2019) Computational investigation of quantum transport to design single-strand DNA logic gate using silicon carbide nanotube electrode. IETE J Res. https://doi.org/10.1080/03772063.2019.1604171
51. Roy P, Dey D, De D (2018) First principle approach towards logic design using hydrogen-doped single-strand DNA. IET Nanobiotechnol 13(1):77–83

52. Dey D, Roy P, De D Implementation of bio-molecular logic gate using DNA and electrically doped GaAs nano-pore: a first principle paradigm. J Mol Model. Springer (IF: 1.346, Accepted, in Production)

53. Anasthasiya ANA, Ramya S, Balamurugan D, Rai PK, Jeyaprakash BG (2018) Adsorption property of volatile molecules on ZnO nanowires: computational and experimental approach. Bull Mater Sci 41(1):4

54. Brahma M, Kabiraj A, Saha D, Mahapatra S (2018) Scalability assessment of Group-IV mono-chalcogenide based tunnel FET. Sci Rep 8(1):1–10

55. Dey D, Roy P, De D (2017) Atomic scale modeling of electrically doped pin FET from adenine based single wall nanotube. J Mol Graph Model 76:118–127

56. Biswal SM, Baral B, De D, Sarkar A (2016) Study of effect of gate-length downscaling on the analog/RF performance and linearity investigation of InAs-based nanowire Tunnel FET. Superlattices Microstruct 91:319–330

57. Zahir A, Pulimeno A, Demarchi D, Roch MR, Masera G, Graziano M, Piccinini G (2016) EE-BESD: molecular FET modeling for efficient and effective nanocomputing design. J Comput Electron 15(2):479–491

58. Gupta SK, Jaiswal GN (2015) Study of Nitrogen terminated doped zigzag GNR FET exhibiting negative differential resistance. Superlattices Microstruct 86:355–362

59. Ghosh RK, Brahma M, Mahapatra S (2014) Germanane: a low effective mass and high bandgap 2-D channel material for future FETs. IEEE Trans Electron Devices 61(7):2309–2315

60. Ghosh RK, Mahapatra S (2013) Proposal for graphene–boron nitride heterobilayer-based tunnel FET. IEEE Trans Nanotechnol 12(5):665–667

61. Lam KT, Liang G (2009) Computational study on the performance comparison of monolayer and bilayer zigzag graphene nanoribbon FETs. In: 2009 13th international workshop on computational electronics. IEEE, pp 1–3

62. Bai P, Chong CC, Li EP, Chen Z (2006) A molecular diode based on conjugated co-oligomers. Int J Nanosci 5(04n05):535–540

63. Khazaei M, Lee SU, Pichierri F, Kawazoe Y (2007) Computational design of a rectifying diode made by interconnecting carbon nanotubes with peptide linkages. J Phys Chem C 111(33):12175–12180

64. Bai P, Lam KT, Li E, Chang KKF (2007) A comprehensive atomic study of carbon nanotube Schottky diode using first principles approach. In: 2007 IEEE international electron devices meeting. IEEE, pp 749–752

65. Li Y, Yao J, Liu C, Yang C (2008) Theoretical investigation on electron transport properties of a single molecular diode. J Mol Struct (Theochem) 867(1–3):59–63

66. Bai P, Li E, Lam KT, Kurniawan O, Koh WS (2008) Carbon nanotube Schottky diode: an atomic perspective. Nanotechnology 19(11):115203

67. Min Y, Yao KL, Liu ZL, Cheng HG, Zhu SC, Gao GY (2009) CrAs (0 0 1)/AlAs (0 0 1) heterogeneous junction as a spin current diode predicted by first-principles calculations. J Magn Magn Mater 321(4):312–315

68. Liu H, Wang N, Li P, Yin X, Yu C, Gao N, Zhao J (2011) Theoretical investigation into molecular diodes integrated in series using the non-equilibrium Green's function method. Phys Chem Chem Phys 13(4):1301–1306

69. El-Hendawy MM, El-Nahas AM, Awad MK (2011) The effect of constitutional and conformational isomerization on the electrical properties of diblock molecular diode. Org Electron 12(6):1080–1092

70. Dey D, De D (2018) A first principle approach toward circuit level modeling of electrically doped gated diode from single wall thymine nanotube-like structure. Microsyst Technol (Springer) 24(7):3107–3121

71. Dai X, Zhang L, Li J, Li H (2017) Metal-semiconductor transition of single-wall armchair boron nanotubes induced by atomic depression. J Phys Chem C 121(46):26096–26101

72. Dey D, Roy P, De D (2019) Electronic transport properties of electrically doped cytosine based optical molecular switch with single-wall carbon nanotube electrodes. IET Nanobiotechnol 13(5):484–492

73. Harada N, Jippo H, Sato S (2017) Theoretical study on high-frequency graphene-nanoribbon heterojunction backward diode. Appl Phys Express 10(7):074001

74. Wang S, Wei MZ, Hu GC, Wang CK, Zhang GP (2017) Mechanisms of the odd-even effect and its reversal in rectifying performance of ferrocenyl-n-alkanethiolate molecular diodes. Org Electron 49:76–84

75. Dey D, Roy P, Purkayastha T, De D (2016) A first principle approach to design gated pin nanodiode. J Nano Res 36:16–30

76. Dey D, Roy P, De D (2016) Electronic characterisation of atomistic modelling based electrically doped nano bio pin FET. IET Comput Dig Tech 10(5):273–285

77. Dey D, Roy P, De D (2017) Design and electronic characterization of bio-molecular QCA: a first principle approach. J Nano Res 49:202–214

78. Geng L, Magyari-Kope B, Nishi Y (2009) Image charge and dipole combination model for the Schottky barrier tuning at the dopant segregated metal/semiconductor interface. IEEE Electron Device Lett 30(9):963–965

79. Chakraverty M, Kittur HM, Kumar PA (2013) First principle simulations of various magnetic tunnel junctions for applications in magnetoresistive random access memories. IEEE Trans Nanotechnol 12(6):977

80. Nadimi E, Planitz P, Ottking R, Wieczorek K, Radehaus C (2010) First principle calculation of the leakage current through $SiO_2$ and $SiO_xN_y$ gate dielectrics in MOSFETs. IEEE Trans Electron Devices 57(3):690–695

81. Geng L, Magyari-Kope B, Zhang Z, Nishi Y (2008) Ab initio modeling of Schottky-barrier height tuning by yttrium at nickel silicide/silicon interface. IEEE Electron Device Lett 29(7):746–749

82. Ghosh RK, Mahapatra S (2012) Direct band-to-band tunneling in reverse biased $MoS_2$ nanoribbon pn junctions. IEEE Trans Electron Devices 60(1):274–279

83. Chakraverty M, Harisankar PS, Gupta K, Ruparelia V, Rahman H (2016) Simulation of electrical characteristics of silicon and germanium nanowires progressively doped to zener diode configuration using first principle calculations. In: Microelectronics, electromagnetics and telecommunications. Lecture notes in electrical engineering, vol 372. Springer, pp 421–428

84. Li J, Gao G, Min Y, Yao K (2016) Half-metallic $YN_2$ monolayer: dual spin filtering, dual spin diode and spin Seebeck effects. Phys Chem Chem Phys 18(40):28018–28023

85. Dey D, De D, Ghaemi F, Ahmadian A, Abdullah LC (2019) Circuit level modelling of electrically doped adenine–thymine nanotube based field effect transistor. IEEE Access 8:6168–6176

86. Dey D, De D (2018) Electrically doped adenine based optical bio molecular pin switch with single walled carbon nanotube electrodes. J Act Passive Electron Devices 13(2–3):107–118

87. Palla P, Ethiraj AS, Raina JP (2016) Resonant tunneling diode based on band gap engineered graphene antidot structures. AIP Conf Proc 1724(1):020069

88. Tabe M, Tan HN, Mizuno T, Muruganathan M, Anh LT, Mizuta H, Nuryadi R, Moraru D (2016) Atomistic nature in band-to-band tunneling in two-dimensional silicon pn tunnel diodes. Appl Phys Lett 108(9):093502

89. Ahmed T, Haraldsen JT, Rehr JJ, Di Ventra M, Schuller I, Balatsky AV (2014) Correlation dynamics and enhanced signals for the identification of serial biomolecules and DNA bases. Nanotechnology 25(12):125705

90. Peng S, Yang Z, Ni X, Zhang H, Ouyang J, Fangping O (2014) DNA translocation through graphene nanopores: a first-principles study. Mater Res Express 1(1):15044

91. Chang P-H, Liu H, Nikolic BK (2014) First-principles versus semi-empirical modeling of global and local electronic transport properties of graphene nanopore-based sensors for DNA sequencing. J Comput Electron 13(4):847–856

92. Guo Y-D, Yan X-H, Xiao Y (2012) Computational investigation of DNA detection using single-electron transistor-based nanopore. J Phys Chem C 116(40):21609–21614

93. Saha KK, Drndic M, Nikolic BK (2012) DNA base-specific modulation of microampere transverse edge currents through a metallic graphene nanoribbon with a nanopore. Nano Lett 12(1):50–55

94. Zhao Q, Wang Y, Dong J, Zhao L, Rui XF, Yu D (2012) Nanopore-based DNA analysis via graphene electrodes. J Nanomater 2012:318950

95. Yang B, Dong R, Yan X, Shi Q (2012) Recognizing nucleosides with transverse electronic transport via perpendicular direction of base planes for DNA sequencing. Nanoscale Res Lett 7(1):512

96. Staykov L, Tsuji Y, Yoshizawa K (2011) Conductance through short DNA molecules. J Phys Chem C 115(8):3481–3490

97. Liu H, Li G, Ai H, Li J, Yuxiang Bu (2011) Electronic enhancement effect of copper modification of base pairs on the conductivity of DNA. J Phys Chem C 115(45):22547–22556

98. Liu H, Li G, Zhang L, Li J, Wang M, Yuxiang Bu (2011) Electronic promotion effect of double proton transfer on conduction of DNA through improvement of transverse electronic communication of base pairs. J Chem Phys 135(13):134315

99. Bagci VMK, Kaun CC (2011) Recognizing nucleotides by cross-tunneling currents for DNA sequencing. Phys Rev E 84(1):11917

100. Li X-F, Ren H, Wang L-L, Cheng K-Q, Yang J, Luo Y (2010) Important structural factors controlling the conductance of DNA pairs in molecular junctions. J Phys Chem C 114(33):14240–14242

101. Banerjee L, Mukhopadhyay A, Sengupta A, Rahaman H (2016) Performance analysis of uniaxially strained monolayer black phosphorus and blue phosphorus n-MOSFET and p-MOSFET. J Comput Electron 15(3):919–930

102. Yamacli S (2014) Extraction of the voltage-dependent quantum capacitance and kinetic inductance of GNRFETs: a first-principles study. J Comput Electron 14(1):249–256

103. Dey D, Roy P, De D (2015 Molecular modeling of nano bio pin FET. In: VLSI design and test (VDAT). IEEE, pp 1–6

104. Dey D, Roy P, De D (2018) First principle study of the self-switching characteristics of the guanine based single optical molecular switch using carbon nanotube electrodes. IET Nanobiotechnol 13(2):237–241

105. Dey D, De D (2018) First principle study of structural and electronic transport properties for electrically doped zigzag single wall GaAs nanotubes. Int J Nano Dimens 9(2):134–144

106. Dey D, Roy P, De D (2016) Nanoscale modeling of molecular nano bio p–i–n tunnel FET with catalytic effect of iron nanofiber. J Nanoeng Nanomanuf 6:9–14

107. Bikshalu K, Manasa MV, Reddy VSK, Reddy PCS, Venkateswara Rao K (2013) Comparison of atomic level simulation studies of MOSFETs containing silica and lantana nanooxide layers. J Nano Electron Phys 5(4):4058

108. Tabe M, Moraru D, Hamid E, Samanta A, Anh LT, Mizuno T, Mizuta H (2013) Dopant-atom-based tunnel SOI-MOSFETs. ECS Trans 58(9):89–95

109. Sengupta A, Ghosh RK, Mahapatra S (2013) Performance analysis of strained monolayer MoS$_2$ MOSFET. IEEE Trans Electron Devices 60(9):2782–2787

110. Mahmoud A, Lugli P (2012) Designing the rectification behavior of molecular diodes. J Appl Phys 112(11):113720–113725

111. Stokbro K, Taylor J, Brandbyge M (2003) Do Aviram–Ratner diodes rectify? J Am Chem Soc 125(13):3674–3675

112. Al-Dirini F, Hossain FM, Mohammed MA, Hossain MS, Nirmalathas A, Skafidas E (2016) Monolayer MoS$_2$ self-switching diodes. J Appl Phys 119(4):044506

113. An Y, Zhang M, Wang T, Wang G, Zhaoming Fu (2016) Rectifications in organic single-molecule diodes alkanethiolate-terminated heterocyclics. Phys Lett A 380(7–8):923–926

114. Pandey SC, Meade R, Sandhu GS (2015) Cu impurity in insulators and in metal-insulator-metal structures: implications for resistance-switching random-access memories. J Appl Phys 117(5):54504

115. Xie F, Fan Z-Q, Liu K, Wang H-Y, Ji-Hai Yu, Chen K-Q (2015) Negative differential resistance and stable conductance switching behaviors of salicylideneaniline molecular devices sandwiched between armchair graphene nanoribbon electrodes. Org Electron 27:41–45

116. Husain MM, Kumar M (2015) Negative differential resistance, rectifying performance and switching behaviour in carbon-chain based molecular devices. Organ Electron Phys Mater Appl 27:92–100

117. Zhang JN, Ma L, Zhang M, Ma LC, Zhang JM (2020) First-principles study of the electronic and optical properties of nitrogen and gold co-doped graphene. Superlattices Microstruct 139:106363

118. Jia X, Zhang H, Zhang Z, An L (2019) First-principles investigation of vacancy-defected graphene and Mn-doped graphene towards adsorption of H2S. Superlattices Microstruct 134:106235

119. Wang S, An Y, Xie C, Zhang H, Zeng Q (2018) First-principles prediction of ferromagnetism in transition-metal doped monolayer AlN. Superlattices Microstruct 122:171–180

120. Cheriyan S, Balamurgan D, Sriram S (2018) Doping effect on monolayer MoS$_2$ for visible light dye degradation-A DFT study. Superlattices Microstruct 116:238–243

121. Luan Z, Zhao L, Chang H, Sun D, Tan C, Huang Y (2017) First-principles study on electronic structures and magnetic properties of Eu-doped phosphorene. Superlattices Microstruct 111:816–823

122. Destefanis GL (1988) Electrical doping of HgCdTe by ion implantation and heat treatment. J Cryst Growth 86(1–4):700–722

123. Lee JS, Shevchenko EV, Talapin DV (2008) Au—PbS core—shell nanocrystals: plasmonic absorption enhancement and electrical doping via intra-particle charge transfer. J Am Chem Soc 130(30):9673–9675

124. Tietze ML, Benduhn J, Pahner P, Nell B, Schwarze M, Kleemann H, Krammer M, Zojer K, Vandewal K, Leo K (2018) Elementary steps in electrical doping of organic semiconductors. Nature Commun 9(1):1–9

125. Dey D, Roy P, De SMIEEE, D (2020) First-principle study of spin transport in GaAs-Adenine-GaAs semi-conductor tunnel junction. In: 2020 IEEE VLSI device circuit and system (VLSI DCS). IEEE, pp 1–5

126. Kienle D, Cerda JI, Ghosh AW (2006) Extended Hückel theory for band structure, chemistry, and transport. I. Carbon nanotubes. J Appl Phys 100(4):043714

127. Kienle D, Bevan KH, Liang GC, Siddiqui L, Cerda JI, Ghosh AW (2006) Extended Hückel theory for band structure, chemistry, and transport. II. Silicon. J Appl Phys 100(4):043715

128. Li P, Wang S, Li J, Wei Y (2012) Structural and optical properties of Co-doped ZnO nanocrystallites prepared by a one-step solution route. J Lumin 132(1):220–225

129. Smialek JL (1988) The effect of sulfur and zirconium co-doping on the oxidation of NiCrAl. High Temp Mater 88:241–254

130. Yang L, Yu J, Wei Z, Li G, Cao L, Zhou W, Chen S (2017) Co-N-doped MoO$_2$ nanowires as efficient electrocatalysts for the oxygen reduction reaction and hydrogen evolution reaction. Nano Energy 41:772–779

131. Chanana A, Mahapatra S (2016) Density functional theory-based study of chlorine doped WS2-metal interface. Appl Phys Lett 108(10):103107

132. Caliskan S, Guner S (2015) First principles study on the spin dependent electronic behavior of Co doped ZnO structures joining the Al electrodes. J Alloys Compd 619:91–97

133. Chauhan SS, Srivastava P, Kurchania R (2011) Half-metallicity in doped armchair graphene nanoribbons—an ab initio approach. J Comput Theor Nanosci 8(4):729–735

134. Salzmann I, Heimel G, Duhm S, Oehzelt M, Pingel P, George BM, Schnegg A, Lips K, Blum RP, Vollmer A, Koch N (2012) Intermolecular hybridization governs molecular electrical doping. Phys Rev Lett 108(3):035502

135. Chai FK, Brews JR, Schrimpf RD, Birnie DP III (1997) Profiling of electrical doping concentration in ferroelectrics. J Appl Phys 82(5):2517–2527

136. Yi J, Lee DH, Lee WW, Park WI (2013) Direct synthesis of graphene meshes and semipermanent electrical doping. J Phys Chem Lett 4(13):2099–2104

137. Lee JH, Lee J, Kim YH, Yun C, Lüssem B, Leo K (2014) Effect of trap states on the electrical doping of organic semiconductors. Org Electron 15(1):16–21

138. Hwang J, Kahn A (2005) Electrical doping of poly (9, 9-dioctylfluorenyl-2,7-diyl) with tetrafluorotetracyanoquinodimethane by solution method. J Appl Phys 97(10):103705

## Publisher's Note